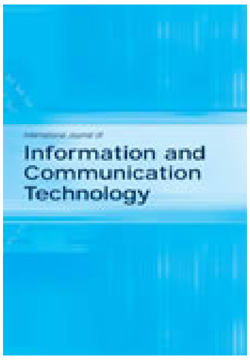

International Journal of Information and Communication Technology

ISSN online: 1741-8070 - ISSN print: 1466-6642
https://www.inderscience.com/ijict

Optimisation of compact UWB circularly polarised antenna

Shanyue Guan, Shiyue Wu, Shaoshuai Liu, Zhiyong Zhao

DOI: 10.1504/IJICT.2025.10071432

Article History:

Received:	15 April 2025
Last revised:	28 April 2025
Accepted:	29 April 2025
Published online:	13 June 2025

Optimisation of compact UWB circularly polarised antenna

Shanyue Guan* and Shiyue Wu

Guizhou Areospace Institute of Measuring and Testing Technology,
Guiyang 550009, China
Email: gsypersonalhk@163.com
Email: wushiy@163.com
*Corresponding author

Shaoshuai Liu

Jiangnan Design Institute of Machinery and Electricity,
Guiyang 550009, China
Email: sshuailiu@163.com

Zhiyong Zhao

Department of Design, Manufacturing and Engineering Management,
University of Strathclyde,
Glasgow G1 1XQ, UK
Email: Zhiyong.zhao@strath.ac.uk

Abstract: This study shows a compact and ultra-wideband (UWB) circularly polarised antenna designed to meet demands of modern wireless communication systems. By incorporating a novel semi-circular slot and innovative decoupling elements, the antenna achieves wideband operation, high isolation, and a miniaturised footprint. Simulations by the software ANSYS HFSS show excellent impedance matching, broad axial ratio bandwidth (ARBW), and stable gain across a wide frequency range. Experimental results further verify its potential for 5G networks and satellite navigation applications. The antenna has a compact structure, high radiation efficiency and effective decoupling strategy, which provides a reference scheme for the further development of wireless communication system.

Keywords: circular polarisation antenna; ultra-wideband; compact; multiple-input multiple-output; MIMO; MIMO technology; neutralisation line decoupling.

Reference to this paper should be made as follows: Guan, S., Wu, S., Liu, S. and Zhao, Z. (2025) 'Optimisation of compact UWB circularly polarised antenna', *Int. J. Information and Communication Technology*, Vol. 26, No. 18, pp.48–64.

Biographical notes: Shanyue Guan received his Master degree form Cardiff University in the UK in 2023. He is currently working at Guizhou Areospace Institute of Measuring and Testing Technology as a Wireless Metrology Engineer. His research interests include microwave communication, antenna calibration and metrology.

Shiyue Wu received his PhD from Sichuan University in June 2022. He is currently working at Guizhou Areospace Institute of Measuring and Testing Technology. His research interests include EMC and HPM research.

Shaoshuai Liu received his Master degree form HongKong University in 2023. He is currently working at Jiangnan design Institute of Machinery and Electricity. His research interests include communication information system.

Zhiyong Zhao received his Master degree form Cardiff University in the United Kingdom in 2023. He is currently studying at the University of Strathclyde in the UK, pursuing a PhD. His research interests include nano-imaging, computer vision, deep learning and wireless and microwave communication.

1 Introduction

As the modern communication era progresses, the rapid evolution of associated technologies has imposed escalating demands on antenna performance, especially for wideband and miniaturisation antennas (Zhu et al., 2023; Zubair et al., 2024). In communication systems, circularly polarised antennas can increase communication capacity, resist multipath and reduce polarisation mismatch. Especially in 5G communications and satellite navigation systems, the miniaturisation and high performance design of circularly polarised antennas are particularly important (Yang et al., 2021; Liu et al., 2023). However, traditional circularly polarised antennas usually suffer from narrow bandwidth and large size, which are difficult to satisfy the requirements of communication systems. Herein, the axial ratio bandwidth (ARBW) defined as the frequency range where the axial ratio remains below 3 dB plays a critical role in ensuring stable circular polarisation purity. A broad ARBW guarantees reliable signal transmission in multipath environments by maintaining consistent polarisation alignment between transmitting and receiving antennas. Consequently, investigation of the ideal design of compact UWB circularly polarised antennas has important theoretical and practical relevance (Yang et al., 2008; Nadeem et al., 2021).

Great achievements have been made in the research on wideband circularly polarised antennas in recent years. Shen et al. (2009) proposed a coplanar waveguide-fed square slit antenna for lower UWB applications. The antenna innovatively protrudes a grounded L-type strip and a small angle at each of corners to achieve circular polarisation. This design exploits the asymmetry of the structure, which makes the antenna exhibit well circular polarisation characteristics. Panahi et al. (2014) proposed printed triangular monopole wideband circularly polarised antenna. This antenna achieves wideband circular polarisation by asymmetrically exciting a planar triangular monopole and a triangular ground plane successfully. This simple and low-cost design opens up a new direction in the development of wideband circularly polarised antennas. Xu et al. (2017) designed microstrip-fed square slit antenna for triple wideband triple-aware circularly polarised radiation. Optimising the grounding structure, which comprises of a frame-type grounding ground and an L-type radiator working in concert, the antenna produces three-band polarised waves. It has good performance in multiple frequency bands, which provides the possibility of multi-band communication and sensing applications. Pan and Dong (2019) proposed three kinds of UWB circularly polarised slot antennas with low profile. By using novel slit shapes and optimised structures, it achieved wideband characteristics and circularly polarised radiation and investigated their performance in detail. Bahrami et al. (2022) proposed reconfigurable UWB circularly polarised antenna which combines a continuously tuned T-type resonator, a bandpass filter and an L-type microstrip line into a reconfigurable feed network. By optimising structure and feed network, the antenna has not only wideband circularly polarised radiation characteristics, but also multiple operating modes and continuous tuning ranges. Song et al. (2024) developed an UWB circularly polarised implantable antenna which can be used to detect blood pressure all the time. The antenna, by designing special slots in the radiating patch and using it in combination with a short needle, provides an effective technical means to realise accurate wireless monitoring inside the human body, which is very significant in the field of medical health. Although the above researches have promoted the development of circularly polarised antennas, the current designs still have problems of limited bandwidth, complex structure, large size, and insufficient performance in the high-frequency band (Ma et al., 2023).

For the problems of circularly polarised antennas, such as narrow bandwidth, large size, and severe mutual coupling in MIMO systems, this study proposes an optimised design for a compact UWB circularly polarised antenna. By introducing a semi-circular slot structure, the A-type antenna is designed and its current distribution is optimised. The axial ratio bandwidth is significantly broadened. The B-type MIMO antenna is formed by mirror-arranging four A-type units. By integrating orthogonal neutralising lines and decoupling patches, coupling between units is suppressed. Through simulation parameter optimisation and experimental validation, the proposed antenna achieves wideband circularly polarised radiation, high isolation, and stable gain within a compact size, proving it suits high-integration wireless systems.

2 Relevant technologies

2.1 Circularly polarised antenna

Antenna radiation can be categorised as either linearly polarised or circularly polarised based on the electric field vector's vibration direction and pattern. Circularly polarised antennas are characterised by a circular rotation of the electric field vector during wave propagation. They exist in two orthogonal states: left-handed (LHCP) and right-handed circular polarisation (RHCP). In practical applications, this antenna provides many benefits including multipath interference suppression and improved communication system robustness (Mak and Luk, 2009; Alnemr et al., 2021).

Mathematically, a circularly polarised wave is designed as a synthesis of two orthogonal linearly polarised waves with a 90° phase difference and equal amplitude. The electric field strength for RHCP waves can be presented as:

$$\mathbf{E}(z,t) = \hat{x}E_0 \cos(\omega t - kz) + \hat{y}E_0 \sin(\omega t - kz) \tag{1}$$

The electric field strength for LHCP waves is:

$$E(z,t) = \hat{x}E_0 \cos(\omega t - kz) - \hat{y}E_0 \sin(\omega t - kz) \tag{2}$$

where E_0 is amplitude, k is wave number, ω is angular frequency and t is time.

To more fully characterise circularly polarised waves, a complex representation can be introduced. It is assumed that the two orthogonal components can be expressed in complex form:

$$E_x = E_0 e^{j(\omega t - kz)} \tag{3}$$

$$E_y = E_0 e^{j(\omega t - kz + \phi)} \tag{4}$$

where ϕ is the phase difference. The direction of rotation and the state of polarisation can be more easily analysed by the complex representation.

The rotation of a circularly polarised wave in space follows the mathematical relation:

$$\mathbf{E}(z,t) = \hat{x}E_x + \hat{y}E_y \tag{5}$$

The performance of circularly polarised antennas is usually represented by following parameters:

- Axial ratio (AR): the axial ratio is a measure of circular polarisation purity. It defines the ratio of the amplitude of long and short axes (Baik et al., 2008). It represents the quality of the circularly polarised wave radiated. The formula for calculating the AR can be expressed as:

  $$AR = \frac{E_{\max}}{E_{\min}} \tag{6}$$

  where $E_{\max}$ and $E_{\min}$ are long-axis and short-axis amplitudes, respectively.

- Bandwidth: bandwidth refers to the frequency spectrum over which an antenna maintains its circular polarisation characteristics (Prasad et al., 2003; Mishra et al., 2022). The frequency range is usually used to define the circular polarisation bandwidth where the AR is less than 3 dB.

- Radiation efficiency: radiation efficiency quantifies the antenna's power conversion capability from input electrical energy to radiated electromagnetic waves (Hashimoto, 2001), which is an important indicator of antenna performance.

To achieve circular polarisation over a wide bandwidth, researchers usually need to optimise the structure and feed network to make sure well circular polarisation characteristics are maintained over a wide bandwidth. Common circularly polarised antennas include slit and microstrip patch antennas, each of which has its own unique design method and application scenario.

2.2 MIMO technology

MIMO technology plays an important role in antenna system design and implementation. The deployment of multiple antennas at both transmitter and receiver can substantial performance enhancement in antenna systems (Bolcskei, 2006). MIMO technology not only increases the spectrum utilisation and system capacity, but enhances the signal anti-interference ability and coverage, compared to traditional single-antenna system. This technique optimally exploits the spatial dimension to achieve both spatial multiplexing and diversity.

MIMO systems use antenna arrays at both transmission and reception sides to process independent data streams, employing advanced signal processing to decode and reconstruct the original signals. The channel capacity is one of the important indexes. It indicates the maximum average data transmission rate the system provides for a given bandwidth and transmit power. The channel capacity follows the mathematical relation (Jerri, 1977):

$$C = B\log_2(1+SNR) \tag{7}$$

where C is channel capacity, B is channel bandwidth and SNR is signal-to-noise ratio. By increasing the number of antennas, the rank of the system can be effectively improved, thus significantly increasing the channel capacity. Furthermore, this technology improves both spectral efficiency and system reliability by implementing spatial multiplexing and diversity techniques. Spatial multiplexing facilitates concurrent transmission of independent data streams in identical spectral resources, achieving significant throughput enhancement through spatial domain utilisation. In contrast, spatial diversity enhances signal reliability and coverage through redundant transmission of identical data across multiple antennas.

MIMO systems often include the following performance parameters:

- Isolation degree: isolation degree serves as a key index for evaluating inter-antenna coupling effects in multi-antenna systems. This index quantifies the power transfer ratio between the transmission port of one antenna and the reception port of another antenna in the array. In practice, an isolation degree greater than 20 dB is typically required to ensure minimal mutual coupling between antennas. Because coupling power above –20 dB degrades MIMO channel capacity and diversity gain. The isolation degree can be expressed as:

  $$Isolation\ (\text{dB}) = 10\log_{10}\left(\frac{P_{received}}{P_{transmitted}}\right) \tag{8}$$

  where $P_{received}$ is the received signal power and $P_{transmitted}$ is the transmitted signal power. The higher the isolation degree, the smaller the coupling between the two antennas, and the more stable the performance of the system. In practice, an isolation degree greater than 20 dB is usually required to ensure that the mutual influence between the antennas is negligible.

- Diversity gain: diversity gain indicates the improvement in bit error rate or SNR of signals received through multiple antennas relative to signals received through a single antenna. Diversity gain is realised by receiver processing techniques such as maximum ratio combining, where the basic idea is to maximise the SNR by summing received signals with optimal weights.

- Envelope correlation coefficient: the envelope correlation coefficient quantifies the statistical independence between received signal envelopes at diversity antenna branches. It defines the ratio of the covariance of two signal envelopes to the product of their standard deviations. The envelope correlation coefficient can be expressed as:

$$\rho = \frac{e\left[|h_1||h_2|\right] - |E[h_1]||E[h_2]|}{\sqrt{E\left[|h_1|^2\right] - |E[h_1]|^2}\sqrt{E\left[|h_2|^2\right] - |E[h_2]|^2}} \tag{9}$$

where h_1 and h_2 are channel gains of two antennas, respectively, $E[\cdot]$denotes the desired value. The envelope correlation coefficient takes values between 0 and 1. When $\rho = 0$, it shows the two signals are uncorrelated and the diversity effect is the best; when $\rho = 1$, it shows the two signals are correlated and the diversity effect is the worst.

3 A-type compact UWB circularly polarised antenna design

3.1 Method of implementing circular polarisation

The generation of UWB circularly polarised waves requires the antenna to be able to simultaneously radiate two orthogonal linearly polarised waves. And these waves have 90° phase difference and the same amplitude. According to this principle, circularly polarised antennas are mainly realised by three methods: the single-feed method, the multiple-feed method, and the multivariate method.

1 Single-feed method

Single-feed method for realising circularly polarised waves usually utilises simple and merged modes of microstrip patch antennas, such as TM_{10} and TM_{01} modes of rectangular microstrip patch antennas. Circularly polarised radiation is enabled by loading a perturbation element on a rectangular microstrip patch antenna. The advantages of the single-feed method are that it does not require a complex feeding network, the antenna structure is simple, the profile is low, and it is well suited for miniaturised system integration by reducing aerodynamic interference and mechanical stress. Thus, it has been widely adopted in the research of wearable circularly polarised antennas. However, the inherent disadvantage of the single-feed method is the narrow bandwidth, which usually needs to be combined with bandwidth spreading techniques to enhance its performance.

2 Multiple-feed method

Multiple-feed method excites the antenna through two or more feed points simultaneously, and the commonly used methods include dual-feed point and quad-feed point. The dual-feed point method utilises two independent feed ports with equal amplitude and phase difference of 90° to excite the antenna, and the feed points are usually located in the orthogonal axes of the patch; while the quad-feed point method utilises four independent feed ports with phase difference of 0°, 90°, 180° and 270° to excite the antenna. Multiple-feed method can obtain an enhanced axial ratio bandwidth along with extended impedance bandwidth, as well as high circular polarisation purity and good cross-polarisation suppression. However, the multiple-feed method requires the introduction of complex feed networks (e.g., power dividers and phase shifters), which can lead to an increase in antenna size and fabrication cost, limiting its use in miniaturised applications.

3 Multivariate method

Multivariate method is based on the idea of array antenna, which forms a rotating antenna array by reasonably arranging multiple independently fed line polarisation units. Each line polarisation unit corresponds to a feed point, which is excited sequentially by parallel or series feeding, and the amplitude between each feed point is kept equal, and the phase difference is 90° sequentially. The multivariate method offers distinct advantages, including broad impedance bandwidth, wide axial ratio bandwidth, effective cross-polarisation suppression, and high gain. However, the disadvantage of the multivariate method is that the antenna occupies a large volume, the structure is complex, and the processing cost is high, which is not conducive to miniaturisation applications. The multivariate method is more suitable for scenarios with higher gain and bandwidth requirements, such as satellite communication or radar systems.

Figure 1 Schematic representation of the three methods of implementing circularly polarised antennas (see online version for colours)

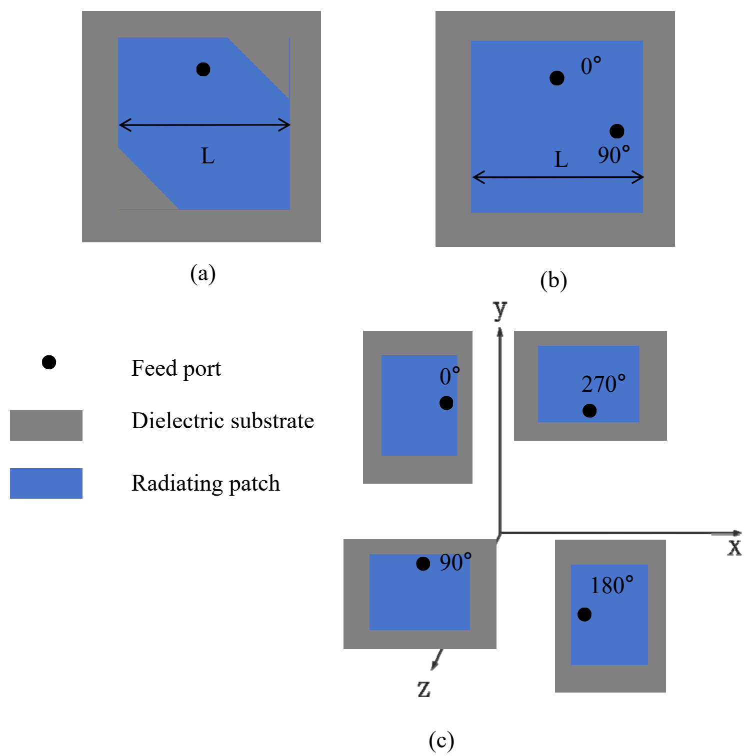

The schematic diagrams of the above three methods are shown in Figure 1. Table 1 demonstrates the advantages and disadvantages of three methods. Considering the characteristics of three methods, the antenna designed by the single-feed method is simple in structure and easy to implement, so the compact UWB circular polarised antenna of A-type designed in this section adopts the single-feed method.

Table 1 Implementation of three circularly polarised antennas

Methodologies	*Advantage*	*Disadvantage*
Single-feed method	1 Simple structure, low production cost 2 Suitable for miniaturised system	1 Inherently narrow bandwidth, need to be combined with bandwidth expansion techniques 2 Circular polarisation bandwidth and axial ratio bandwidth are limited
Multiple-feed method	1 Wide axial bandwidth and impedance bandwidth can be realised 2 High purity of circular polarisation, good suppression of cross-polarisation	1 Need for complex feeder networks 2 Large antenna size
Multivariate method	1 Wide impedance bandwidth and axial bandwidth can be realised 2 Good cross-polarisation suppression, high gain	1 Complex structure and high processing cost 2 Not suitable for miniaturised applications.

3.2 A-type antenna structure design

Figure 2 shows the diagram of the A-type antenna. The A-type compact UWB circularly polarised antenna is the core original radiating component of the B-type antenna, and the antenna elements are fabricated on a 20 × 20 × 1.6 mm^3 FR-4 dielectric substrate.

In the first step, the antenna adopts a traditional rectangular microstrip feeding structure, and a square slot structure change is used to optimise the current path and resonant frequency band, redistributing phase-shifted orthogonal currents to achieve 90° phase difference. In the second step, to achieve circularly polarised radiation of the antenna, two rectangular patches are designed to establish a 90° phase difference, which also results in a shift of the antenna resonance frequency towards higher frequencies. Therefore, in the third step, a semicircular slot is etched on the right part of the rectangular strip, and the new semicircular slot structure leads to further optimisation of the antenna performance. In this, both the antenna's fundamental resonant frequency and axial ratio bandwidth are shifted toward lower frequencies.

Using ANSYS HFSS to design the A-type antenna. It is found to resonate in the 2.76–4.29 GHz band with a 3-dB ARBW of about 522 MHz (3.155–3.677 GHz). Apparently, the antenna's low-frequency operation is attained by etching a semicircular slot in the rectangular patch. This modification results in a 250 MHz downward shift in resonant frequency and a concurrent 190 MHz reduction in axial ratio frequency. To obtain the optimal antenna dimensions, the semicircular groove dimensions R on the ground of the antenna at are analysed comparatively and it is found that R is the key parameter affecting the impedance matching, and the change of R influences the surface current amplitude distribution on the antenna, and the adjustments of the amplitude of the current of the various structures induces phase-variant vector recombination of current flows, leading to directional variation in the superposed current. The antenna's resonant frequency shifts toward the low frequency. Through simulation and comparison, it is determined that the optimal S_{11} parameter and axial ratio are obtained when R = 3.5 mm. The A-type antenna lays the foundation for the design of the B-type antenna, and dimensions of the A-type compact UWB circularly polarised antenna are shown in Table 2.

Figure 2 Structure diagram of the A-type compact UWB circularly polarised antenna (see online version for colours)

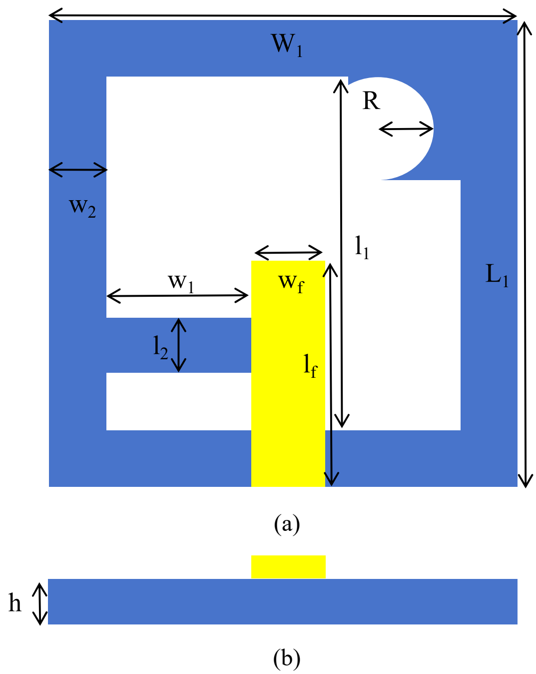

Table 2 Dimensions of A-type compact UWB circularly polarised antenna

Parameters	*Size (mm)*
L_1	20
W_1	20
l_1	17
l_2	2.5
w_f	2.5
l_f	10
h	1.6
w_1	6
w_2	2

4 B-type compact UWB circularly polarised antenna design

4.1 MIMO antenna coupling

In an ideal MIMO system, each antenna is completely independent. However, in reality, the antennas in a MIMO system are mutually coupled and cannot be regarded as working independently (Nadeem and Choi, 2018). Therefore, effective coupling reduction between antenna elements is important for the system. For traditional MIMO antennas with large spacing, the influence of mutual coupling is small, but to miniaturised antennas, the enhancement of mutual coupling is particularly important to ensure that the antenna units still have low mutual coupling and good radiation performance in a compact space.

MIMO antenna units produce strong electromagnetic mutual coupling between the main reasons are: near-field space waves, floor current and dielectric surface waves. The effect of near-field space waves arises from the electromagnetic waves radiated by one unit, which induce currents on neighbouring units' radiation structures. When the antenna operates, the ground plane generates a corresponding current distribution. This current distribution can couple energy from one unit's port to a neighbouring unit's port, leading to degraded isolation between the units. Additionally, dielectric surface waves propagate along the substrate surface and can similarly couple electromagnetic energy from one unit to neighbouring units.

Figure 3 Neutralisation line decoupling schematic (see online version for colours)

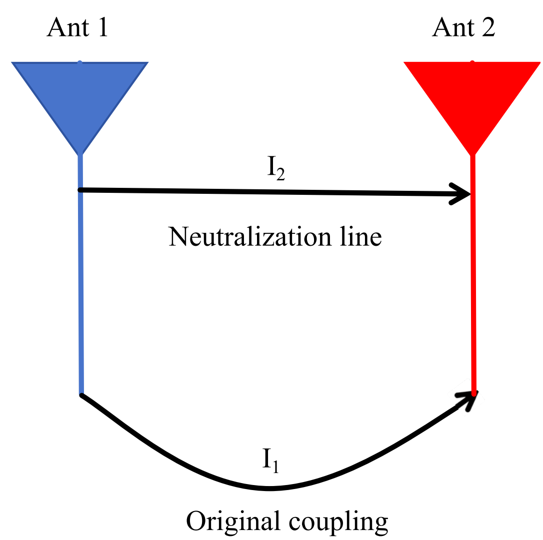

To minimise inter-antenna coupling effects, the B-type compact UWB circularly polarised antenna designed in this paper employs the neutralisation line decoupling method. The neutralisation line is a microstrip line structure placed between two antenna units, which can improve the isolation, and its schematic diagram is shown in Figure 3. I_1 is the original coupling wave path from antenna 1 to antenna 2, and I_2 is the coupling wave path from antenna 1 to antenna 2 after the neutralisation line. Through controlling the position and size of the neutralising line, the amplitude of the electromagnetic wave in the coupling path I_1 and the electromagnetic wave in the coupling path I_2 are equal in amplitude and opposite in phase. Then the coupling between the two antennas can cancel each other, thus improving the isolation degree of the sky unit.

To study the neutralisation line model, the neutralisation line is equivalent to a characteristic impedance connected in parallel to the MIMO antenna, which changes the conductance matrix of the antenna. According to the relationship between the conductance and the desired frequency, the approximate size of the neutralisation line can be obtained. Finally, HFSS is used to adjust and optimise the structure of the neutralisation line. The antenna unit is then expressed as:

$$Y^A = \begin{bmatrix} \dfrac{1-\alpha^2}{1+\alpha^2} & \dfrac{j2\alpha}{1+\alpha^2} \\ \dfrac{j2\alpha}{1+\alpha^2} & \dfrac{1-\alpha^2}{1+\alpha^2} \end{bmatrix} \tag{10}$$

Assuming, the characteristic impedance is Z_d and the length is L_d, the corresponding conductance matrix can be obtained by paralleling the neutralisation line into the MIMO system:

$$Y^D = \begin{bmatrix} -\dfrac{j\cot(\beta L_d)}{Z_d} & \dfrac{j}{Z_d \sin(\beta L_d)} \\ \dfrac{j}{Z_d \sin(\beta L_d)} & -\dfrac{j\cot(\beta L_d)}{Z_d} \end{bmatrix} \tag{11}$$

where β denotes the phase constant.

$$\beta = \frac{2\pi}{\lambda} \tag{12}$$

Adding the conductance matrix of the antenna unit to the conductance matrix of the neutralisation line gives the following result:

$$Y_{21} = Y_{21}^A(w) + Y_{21}^D(w) \approx 0 \tag{13}$$

Therefore, the reduction of the compact UWB circularly polarised antenna coupling can be achieved by neutralising the line.

4.2 B-type antenna structure design

4.2.1 Structural design.

Figure 4 shows the design flowchart of the B-type antenna. The B-type circularly polarised antenna consists of four A-type circularly polarised antennas located on the substrate, and the spacing between the radiating elements is $0.057\lambda_0$ (with a centre frequency of f_c = 3.45 GHz) to maintain the antenna elements. The antenna generates right-hand circular polarisation under port 1/4 excitation, while producing left-hand circular polarisation when ports 2/3 are energised.

Figure 4 The design flowchart of the B-type compact UWB circularly polarised antenna (see online version for colours)

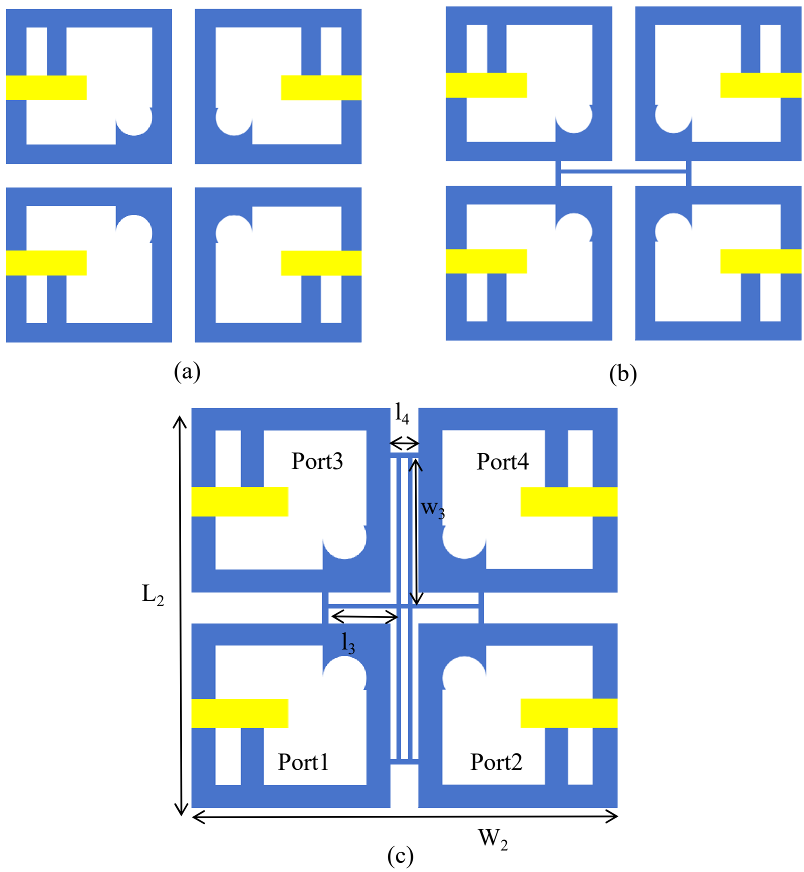

To achieve wide axial ratio bandwidth and enhanced port isolation, the circularly polarised antenna elements are configured in mirrored symmetry about the central plane. In Figure 4(a), a spacing of 5 mm is designed between the antenna units to maintain the impedance bandwidth and to minimise the mutual influence. Then, in Figure 4(b), an I-type strip is introduced between the antenna units as a decoupling element, which restores the circular polarisation performance and further improves the isolation between ports. However, the narrower axial ratio bandwidth and mismatched resonant frequencies are still problems that need to be solved. Therefore, in Figure 4(c), a new II-type strip patch is introduced between the antenna units as a decoupling element. The II-type structure patch restores the circular polarisation property to a larger extent through phase-dependent current vector reorientation across antenna elements. The introduction of the II-type structure makes the circular polarisation property significantly improved with respect to that of a single antenna unit. The decoupling structure employs orthogonally connected I-type and II-type metal strips as neutralisation lines. By altering the current phase distribution across antenna units, the neutralising currents oppose and cancel the original coupled currents, thereby reducing inter-element coupling and preserving the antenna's circular polarisation characteristics.

4.2.2 Structural optimisations

To further study the performance of the B-type antenna. The core dimensions of the decoupling structure of the antenna, l_3 and w_3, are parametrically analysed by using the electromagnetic simulation software ANSYS HFSS, where l_3 represents the length of the I-type strip and w_3 represents the length of the II-type strip. By changing one design parameter while keeping another parameter unchanged, the S_{11} parameters of the antenna are observed and the optimum size of the decoupled structure is obtained through optimisation.

Figures 5(a) and 5(b) respectively demonstrate the variation of S_{11} parameters with the length of I-type metal strip and the variation of S_{11} parameters with the length of II-type metal strip. It is observed that the S_{11} parameters become smaller and then gradually larger in the range of 2.6–4.3 GHz. For comparison, it is found that the S_{11} parameter is minimised with a value of –43.26 dB when l_3 is 7 mm and w_3 is 17.5 mm, which corresponds to a frequency of 3.44 GHz.

Figure 5 Variation of S_{11} parameter with length of metal strip for I and II shapes, l_3 and w_3 (see online version for colours)

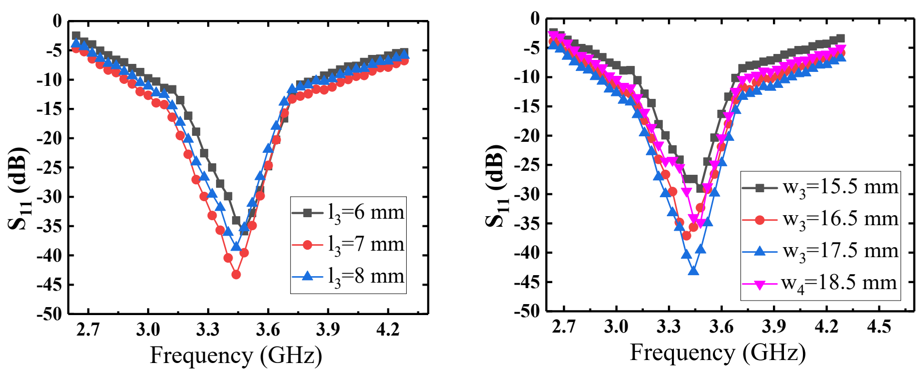

(a) (b)

Through structural optimisation, the dimensional parameters of the final B-type compact UWB circularly polarised antenna are obtained as shown in Table 3.

Table 3 Dimensions of B-type compact UWB circularly polarised antenna

Parameters	*Size (mm)*
L_2	45
W_2	45
l_3	7
l_4	5
w_3	17.5

5 Experimental results and analyses

The proposed B-type compact UWB circularly polarised antenna is processed and tested to further verify the reliability of the design. The size of B-type antenna is 45 × 45 × 1.6 mm^3, which possesses compact characteristics. The proposed decoupling structure is an all-metal structure, and the antenna is fed using a rigid coaxial cable with an SMA male connector. Tests are performed on the S_{11} parameters, axial ratio bandwidth, and gain of the B-type antenna.

5.1 S_{11} parameters

The S_{11} parameters are measured by using a vector network analyser (VNA). Figure 6 shows the test and simulation results. It is observed that the B-type antenna operates in frequency range of 2.92–3.96 GHz, a total of 1,040 MHz, below –10 dB. In the figure, the antenna's simulation deviates slightly from the measured data, but the overall trend matches. This discrepancy may arise from manufacturing tolerances in the millimetre-scale antenna structure. Therefore, the measured results show that the S_{11} parameters meet the requirements.

Figure 6 Simulation and test results of S_{11} parameters of the B-type compact UWB circularly polarised antenna (see online version for colours)

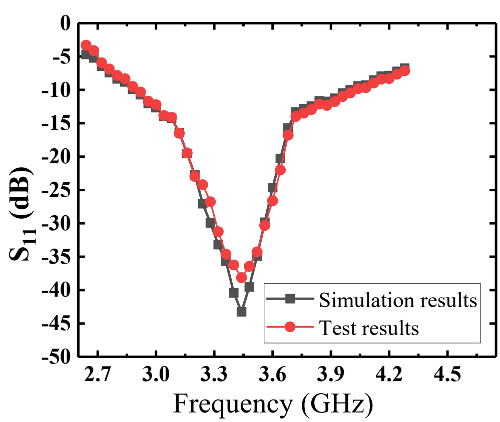

5.2 Axial ratio bandwidth and gain

Figure 7(a) shows the relationship between axial ratio and frequency of B-type compact UWB circularly polarised antenna, and Figure 7(b) shows the relationship between the gain and frequency. The simulation results of both plots are in general agreement with the test results with the same trend. The test results show that the frequency range that satisfies the AE ≤ 3 dB is 2.8–4.04 GHz, within the frequency band 2.92–3.96 GHz of the MIMO antenna S_{11} parameter, the range of the measured gain is 2.92–7.73 dBi. The ARBW is calculated by the formula:

$$ARBW\ (\%) = \frac{f_{high} - f_{low}}{f_{centre}} \times 100\% \tag{14}$$

$$f_{centre} = \sqrt{f_{low} \times f_{high}} \tag{15}$$

where f_{high} is the upper limit frequency, f_{low} is the lower limit frequency, and f_{centre} is the geometric mean centre frequency. After calculation, the ARBW of the B-type compact UWB circularly polarised antenna is obtained to be 36.4%, which has better circularly polarised performance with wide bandwidth characteristics.

Figure 7 Simulation and test results of the axial ratio and gain of the B-type compact UWB circularly polarised antenna, (a) axle ration (b) gain (see online version for colours)

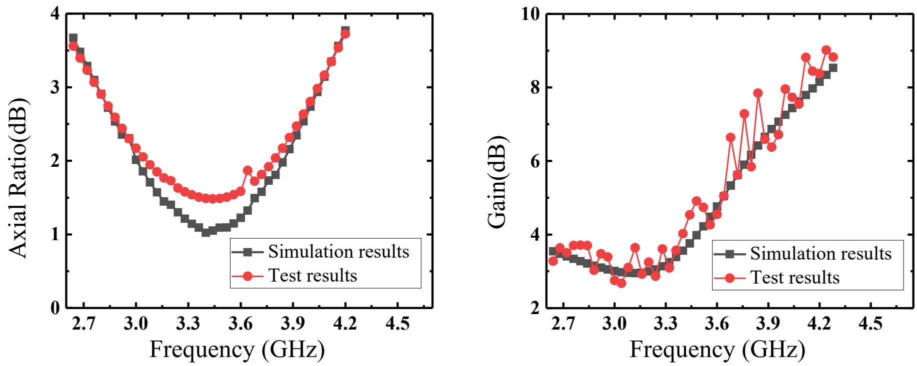

(a) (b)

6 Conclusions

This research proposes a B-type compact UWB circularly polarised antenna and optimises its design to meet the demands for high performance, miniaturisation, and wideband operation. By introducing innovative designs such as semicircular slots and decoupling structures, the antenna excels in impedance matching, ARBW and mutual coupling suppression in MIMO configurations. The designed antenna exhibits excellent circular polarisation characteristics over a wide frequency band and is suitable for application scenarios such as 5G communication and satellite navigation. The main contribution is to propose a compact antenna structure that can significantly reduce the antenna size while maintaining high radiation efficiency and polarisation purity. By adopting the decoupling technique of neutralisation lines, the mutual coupling between antenna units is effectively reduced to make sure system operational stability. Additionally, the optimised design of the feed network and grounding layer further improves the antenna's wideband performance and gain stability. Experimental results verify that designed antenna shows good performance consistent with the simulation analysis in the actual test, which verifies its feasibility and practicality. The design not only overcomes the limitations of traditional circularly polarised antennas such as narrow bandwidth and large size, but also provides a scalable framework for antenna design in compact wireless devices.

Declarations

All authors declare that they have no conflicts of interest.

References

Alnemr, F., Ahmed, M.F.a. and Shaalan, A.A. (2021) 'A compact 28/38 GHz MIMO circularly polarized antenna for 5 G applications', *Journal of Infrared, Millimeter, and Terahertz Waves*, Vol. 42, pp.338–355.

Bahrami, S., Moloudian, G., Song, H-J. and Buckley, J.L. (2022) 'Reconfigurable UWB circularly polarized slot antenna with three modes of operation and continuous tuning rang', *IEEE Transactions on Antennas and Propagation*, Vol. 70, No. 9, pp.8542–8547.

Baik, J-W., Lee, K-J., Yoon, W-S., Lee, T-H. and Kim, Y-S. (2008) 'Circularly polarised printed crossed dipole antennas with broadband axial ratio', *Electronics Letters*, Vol. 44, No. 13, pp.785–786.

Bolcskei, H. (2006) 'MIMO-OFDM wireless systems: basics, perspectives, and challenges', *IEEE Wireless Communications*, Vol. 13, No. 4, pp.31–37.

Hashimoto, N. (2001) 'Measurement of sound radiation efficiency by the discrete calculation method', *Applied Acoustics*, Vol. 62, No. 4, pp.429–446.

Jerri, A.J. (1977) 'The Shannon sampling theorem – its various extensions and applications: a tutorial review', *Proceedings of the IEEE*, Vol. 65, No. 11, pp.1565–1596.

Liu, T., Liu, L., Chen, H., Sun, H., Jin, Z., Chernogor, L.F., Batrakov, D.O. and Sun, Z. (2023) 'A broadband circularly polarized antenna based on transparent conformal metasurface', *IEEE Antennas and Wireless Propagation Letters*, Vol. 22, No. 12, pp.3197–3201.

Ma, W., Zhu, L. and Zhang, R. (2023) 'Compressed sensing based channel estimation for movable antenna communications', *IEEE Communications Letters*, Vol. 27, No. 10, pp.2747–2751.

Mak, K.M. and Luk, K.M. (2009) 'A circularly polarized antenna with wide axial ratio beamwidth', *IEEE Transactions on Antennas and Propagation*, Vol. 57, No. 10, pp.3309–3312.

Mishra, B., Verma, R.K. and Singh, R.K. (2022) 'A review on microstrip patch antenna parameters of different geometry and bandwidth enhancement techniques', *International Journal of Microwave and Wireless Technologies*, Vol. 14, No. 5, pp.652–673.

Nadeem, I. and Choi, D-Y. (2018) 'Study on mutual coupling reduction technique for MIMO antennas', *IEEE Access*, Vol. 7, pp.563–586.

Nadeem, I., Alibakhshikenari, M., Babaeian, F., Althuwayb, A.A., Virdee, B.S., Azpilicueta, L., Khan, S., Huynen, I., Falcone, F. and Denidni, T.A. (2021) 'A comprehensive survey on 'circular polarized antennas' for existing and emerging wireless communication technologies', *Journal of Physics D: Applied Physics*, Vol. 55, No. 3, p.033002.

Pan, Y. and Dong, Y. (2019) 'Low-profile low-cost ultra-wideband circularly polarized slot antennas', *IEEE Access*, Vol. 7, pp.160696–160704.

Panahi, A., Bao, X., Ruvio, G. and Ammann, M. (2014) 'A printed triangular monopole with wideband circular polarization', *IEEE Transactions on Antennas and Propagation*, Vol. 63, No. 1, pp.415–418.

Prasad, R., Dovrolis, C., Murray, M. and Claffy, K. (2003) 'Bandwidth estimation: metrics, measurement techniques, and tools', *IEEE Network*, Vol. 17, No. 6, pp.27–35.

Shen, Y., Law, C.L. and Shen, Z. (2009) 'A CPW-FED circularly polarized antenna for lower ultra-wideband applications', *Microwave and Optical Technology Letters*, Vol. 51, No. 10, pp.2365–2369.

Song, Z., Zheng, X., Shi, Y. and Wang, Y. (2024) 'Implantable small ultra-wideband circularly polarized antenna design for continuous blood pressure monitoring', *Scientific Reports*, Vol. 14, No. 1, p.25199.

Xu, R., Li, J., Qi, Y-X., Guangwei, Y. and Yang, J-J. (2017) 'A design of triple-wideband triple-sense circularly polarized square slot antenna', *IEEE Antennas and Wireless Propagation Letters*, Vol. 16, pp.1763–1766.

Yang, S-L.S., Kishk, A.A. and Lee, K-F. (2008) 'Wideband circularly polarized antenna with L-shaped slot', *IEEE Transactions on Antennas and Propagation*, Vol. 56, No. 6, pp.1780–1783.

Yang, Y., Ban, Y-L., Yang, Q., Lian, J-W., Sun, Q. and Wu, G. (2021) 'Millimeter wave wide-angle scanning circularly polarized antenna array with a novel polarizer', *IEEE Transactions on Antennas and Propagation*, Vol. 70, No. 2, pp.1077–1086.

Zhu, L., Ma, W. and Zhang, R. (2023) 'Modeling and performance analysis for movable antenna enabled wireless communications', *IEEE Transactions on Wireless Communications*, Vol. 23, No. 6, pp.6234–6250.

Zubair, M., Jabbar, A., Tahir, F.A., Kazim, J.u.R., Rehman, M.U., Imran, M., Liu, B. and Abbasi, Q.H. (2024) 'A high-performance sub-THz planar antenna array for THz sensing and imaging applications', *Scientific Reports*, Vol. 14, No. 1, p.17030.